Supporting Information: **Cation Gating and Relocation during the Highly Selective 'Trapdoor' Adsorption of CO_2 on Univalent Cation forms of Zeolite Rho**

Magdalena M. Lozinska,[1] John P. S. Mowat,[1] Paul A. Wright,[1,*] Stephen P. Thompson,[2] Jose L. Jorda,[3] Miguel Palomino,[3] Susana Valencia[3] and Fernando Rey[3]

[1] *EaStCHEM School of Chemistry, University of St Andrews, Purdie Building, North Haugh, St Andrews, Fife, KY16 9ST, Scotland,* paw2@st-andrews.ac.uk; [2] *Diamond Light Source Ltd, Harwell Science and Innovation Campus, Didcot, Oxfordshire, OX11 0DE, UK;* [3] *Instituto de Tecnología Química (UPV-CSIC), Universidad Politécnica de Valencia, Consejo Superior de Investigaciones Científicas, Avenida de los Naranjos s/n, 46022 Valencia, Spain*

Contents

S1. Experimental details of synthesis and ion exchange of Na,Cs-Rho and K-chabazite

S1.1. Synthesis of Na,Cs-Rho – Zeolite Na,Cs-Rho was synthesized from the gel composition: 1.8 Na_2O : 0.3 Cs_2O: 1.0 Al_2O_3 : 10 SiO_2 : 0.5 (18-crown-6) : 100 H_2O, according to published procedures.[1,2] The starting mixture was prepared by dissolving 1,4,7,10,13,16-hexaoxacyclooctadecane (18-crown-6; $C_{12}H_{24}O_6$; 1.12g;; ≥99%; Sigma-Aldrich), cesium hydroxide (CsOH; 0.75g; 99.9%; Sigma-Aldrich) and sodium hydroxide (NaOH; 0.33g; 98.5%; Fisher Chemicals) in distilled water (6.7 mL). Sodium aluminate ($NaAlO_2$; 2.21g; 31% Na_2O, 38,5% Al_2O_3; BDH Chemicals Ltd.) followed by colloidal silica, Ludox AS-40 (12.5g; 40%, suspension in water; Sigma-Aldrich) was added and the mixture stirred until homogeneous. The gel formed was aged at room temperature for 24 hours in a closed polypropylene bottle under continuous stirring. The crystallization was carried out under static conditions in the same closed polypropylene bottle for 8 days at 383 K. After reaction, the solid obtained was filtered, washed with distilled water then dried at 373 K overnight. The as-prepared Na,Cs-Rho was heated at 823 K under oxygen for 12 hours to remove the template.

S1.2. Ion exchange and determination of the unit cell composition of Na,Cs-Rho – Ion exchange of Na,Cs-Rho was conducted according to published procedures.[2-6] The calcined Na,Cs-Rho was fully exchanged with 10% NH_4Cl solution (99.9%; Alfa Aesar) and then with 10% nitrate solutions of Na, Cs and K (99.5-99.9%; Sigma-Aldrich) at 353 K in a round bottom flask with condenser. In all cases cation exchange was continued until EDX indicated the exchange was complete.

The unit cell compositions of all Rho samples were estimated from a combination of EDX analysis and MAS NMR spectroscopy. EDX analysis was performed in a JEOL JSM 5600 SEM, with an Oxford INCA Energy 200 EDX analyser. Solid-state ^{29}Si MASNMR was performed using a Varian VNMRS spectrometer operating at 79.44 MHz for ^{29}Si. Deconvolution of the ^{29}Si MASNMR of the as-prepared Na,Cs-Rho, in which all aluminium occupies tetrahedral sites and all tetrahedral sites are crystallographically equivalent, was used to determine the framework Si/Al ratio of zeolite Rho and used to calibrate the Si/Al ratios determined via EDX. The Si/Al ratio measured in the as-prepared zeolite Rho was obtained by EDX as 4.0 and by deconvolution of the ^{29}Si MAS NMR spectrum as 3.9. The NMR value was taken as the more accurate, and compositions calculated accordingly for all

Rho materials. Full details of the composition of cation-exchanged zeolites are given in a table below.

Table S1.1 Unit Cell Compositions determined by EDX.

Sample	Atomic % from EDX						Unit cell formula of dehydrated sample
	O	Si	Al	Na	Cs	K	
Na,Cs-Rho	68 ± 1	21 ± 1	5 ± 1	4 ± 0.5	2 ± 0.5	N.D.	$Na_{6.8}Cs_{3.0}Al_{9.8}Si_{38.2}O_{96}$
Na-Rho	70 ± 1	20 ± 1	5 ± 1	5 ± 1	N.D.	N.D.	$Na_{9.8}Al_{9.8}Si_{38.2}O_{96}$
Cs-Rho	68 ± 1	20 ± 1	5 ± 1	N.D.	7 ± 1	N.D.	$Cs_{9.8}Al_{9.8}Si_{38.2}O_{96}$
K-Rho	67 ± 1	21 ± 1	5 ± 1	N.D.	N.D.	6 ± 1	$K_{9.8}Al_{9.8}Si_{38.2}O_{96}$

Values for oxygen are semi-quantitative
N.D. – not detected

S1.3. Synthesis of K-chabazite – Zeolite K-chabazite was synthesized from the gel composition: 2.65 K_2O: 1.0 Al_2O_3: 4.8 SiO_2 : 183 H_2O, according to a published procedure.[7] Na-Y zeolite (CF-900; 8g; 0.70 mmol; Crosfield) was exchanged by mechanical stirring for 24 hours at 353 K with 2 M ammonium chloride solution (NH_4Cl; 99.9%; Alfa Aesar). The mixture was filtered and to the filtrate a new volume of NH_4Cl was added. The procedure was repeated five times, and the NH_4-Y was dried at 373 K overnight and heated at 823 K, to remove NH_3, leaving the protonic form of zeolite Y. H-Y was then suspended in distilled water (64 mL) and an aqueous solution of potassium hydroxide (KOH; 9g; 98.5%; Fisher Chemicals) was added. The mixture was stirred for 1 hour, and then was transferred into a polypropylene bottle. The gel was heated in the oven at 368 K for 4 days and the solid product was recovered by filtration, washed with distilled water, and dried at 373 K.

S2. Detailed description of measurement of CO_2 and CH_4 isotherms

The adsorption isotherms in the pressure range up to 900 kPa were measured in an IGA-3 gravimetric analyzer (Hiden Isochema) using approximately 50 mg of sample, that were placed in the balance and outgassed at 673 K under vacuum during 4 h before each adsorption experiment. The temperature of the sample was subsequently reduced under vacuum until the target temperature (between 283 K and 333 K) was reached. The CO_2 and CH_4 adsorption measurements were performed by introducing gas to build up the desired pressures into the gravimetric system. The equilibrium conditions were fixed at 98% of the calculated uptake using the Avrami-Erofe'ev model or a maximum equilibration time of 120 min for each point of the isotherm. Selected adsorption isotherms in the low pressure range were measured in a Micromeritics ASAP 2010 instrument using approximately 150 mg of adsorbent placed in a sample holder that was immersed into a liquid circulation thermostatic bath for precise temperature control. Before each measurement, the sample was treated overnight at 673 K under vacuum. Adsorption isotherms were then acquired at 283, 298, 313 and 333 K.

For Na-Rho, the high pressure (gravimetric) and low pressure (volumetric) isotherms at each temperature were combined (see Figure S2.1)

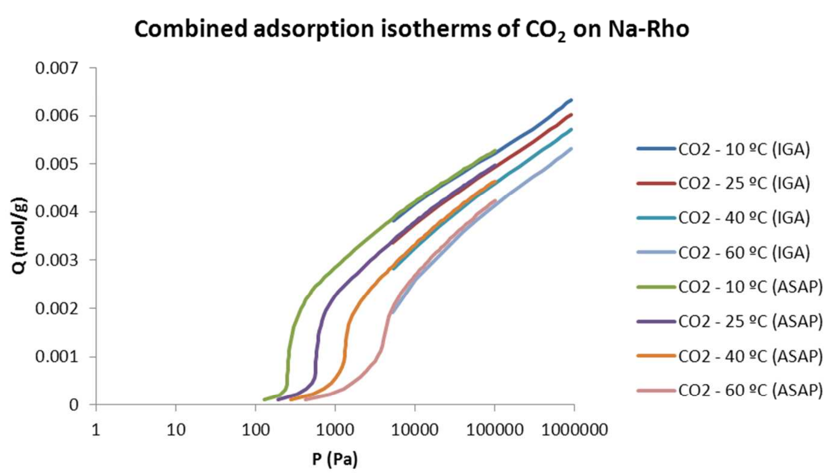

Figure S2.1. Adsorption isotherms of CO_2 on Na-Rho, determined by combining low pressure data measured volumetrically and high pressure data measured gravimetrically.

These combined isotherms were fitted using a Virial-type equation and the differential isosteric heat of CO_2 adsorption (q_{st}) was calculated at different coverages from the fitted isotherms by applying the Clausius-Clapeyron equation:

$$q_{st} = R \cdot T^2 \cdot \left[\frac{\partial(\ln P)}{\partial T}\right]_{Q_i} \equiv R \cdot \left[-\frac{\partial(\ln P)}{\partial\left(\frac{1}{T}\right)}\right]_{Q_i}$$

The isosteric heats of adsorption are given as a function of loading below.

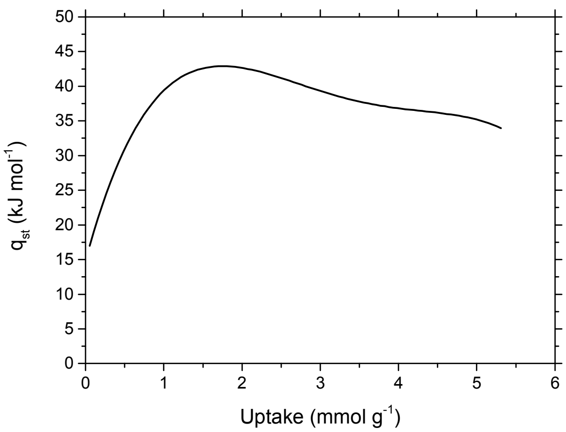

Figure S2.2. The isosteric heat of adsorption of CO_2 on Na-Rho, q_{st}, as a function of uptake, calculated from adsorption isotherms at 283, 298, 313 and 333 K.

S3. Calorimetric measurements

The heat of adsorption of CO_2 was determined by calorimetric adsorption measurements performed on a Sensys-Evo Calorimeter from Setaram equipped with a thermogravimetric accessory.

The partial pressure of CO_2 was modified by mixing CO_2 in He using appropriate gas flow controllers at the entrance of the calorimetric instrument. Prior to each adsorption experiment, the sample was dehydrated by flowing He at 673 K for 2 hours and then cooled down to 303 K (selected as adsorption temperature). Once the temperature was stable, the selected CO_2/He flow was put in contact with the sample and the evolved heat of adsorption was continuously measured. Typical plots of these measurements are shown below:

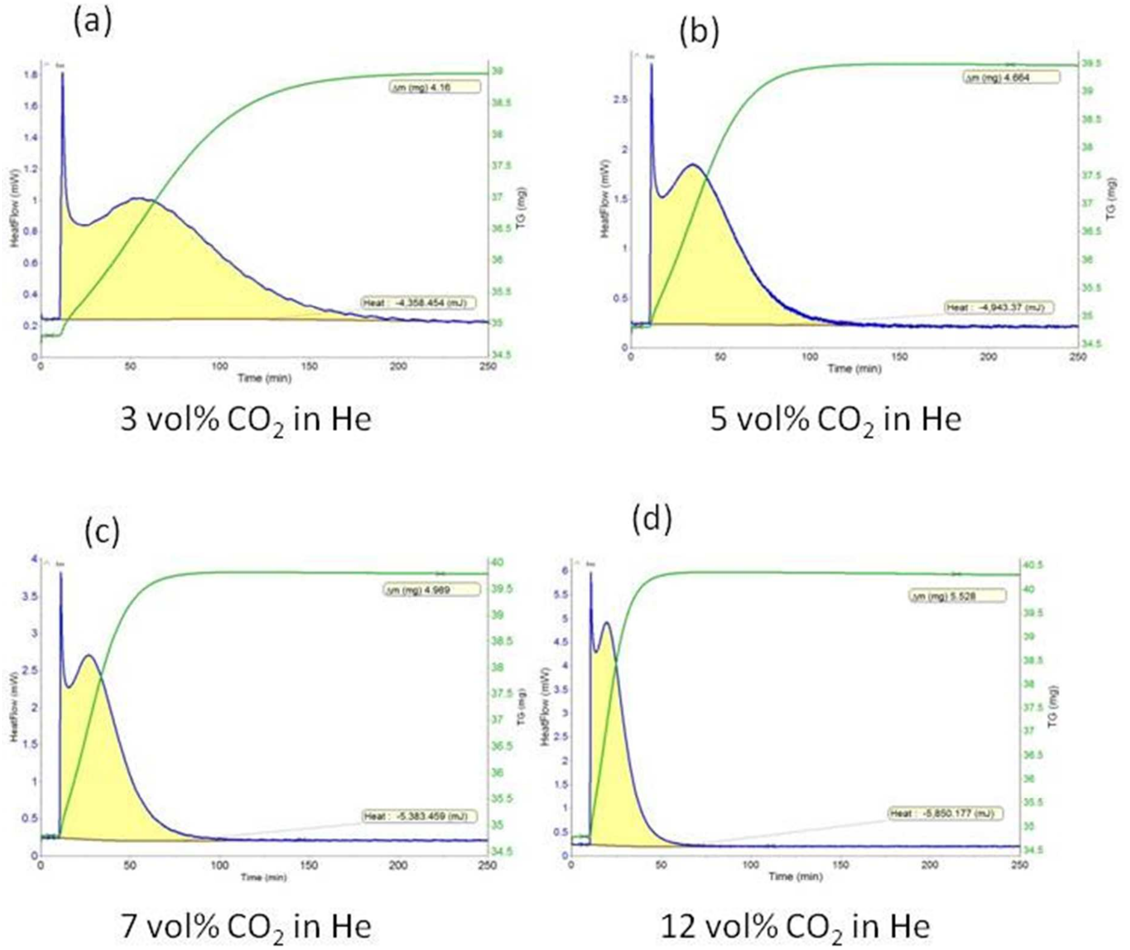

Figure S3.1. Heats of adsorption measured by calorimetry as CO_2/He gas mixtures with different CO_2 contents are passed over Na-Rho and the evolved heat (blue curve, yellow area) and CO_2 uptake (green curve) are measured.

S4. *In situ* synchrotron PXRD of Na-Rho during CO_2 adsorption

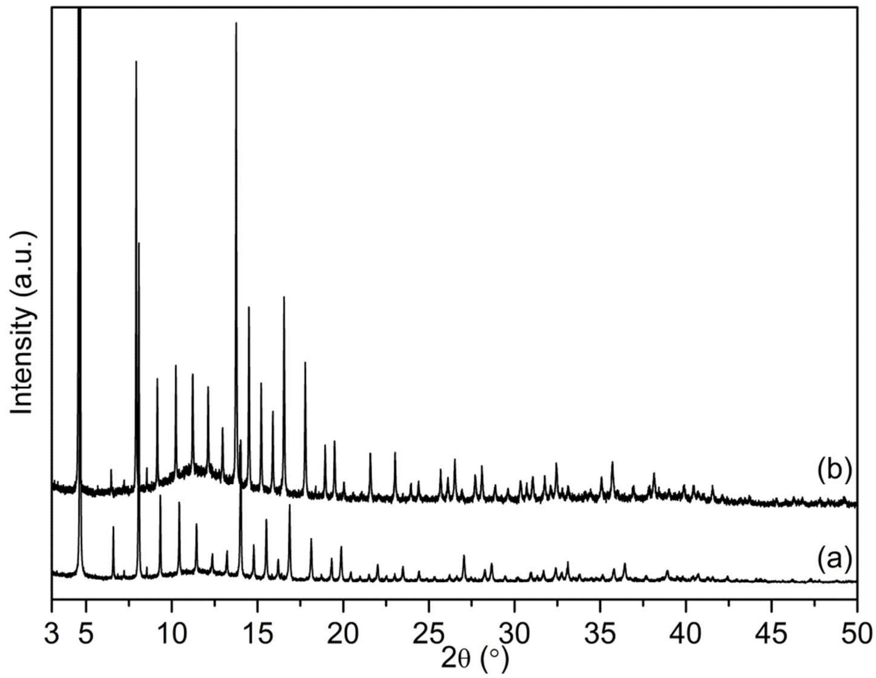

Figure S4.1 *In situ* synchrotron PXRD (λ = 0.827159(2) Å) of Na-Rho during CO_2 adsorption. (a) Sample dehydrated at 723 K and cooled down to RT and (b) sample in equilibrium with 1 bar of CO_2. The (offset) patterns have been collected at 298 K using the same operating conditions.

S5. Crystallographic details of the refined dehydrated Na-Rho, Cs-Rho, K-Rho and K-chabazite and those solids with adsorbed CO_2

Table S5

	Na-Rho	**Na-Rho (1 bar CO_2)**	**Cs-Rho**	**Cs-Rho (4 bar CO_2)**
Unit cell	$Na_{9.8}Al_{9.8}Si_{38.2}O_{96}$	$Na_{9.8}Al_{9.8}Si_{38.2}O_{96}\cdot 12CO_2$	$Cs_{9.8}Al_{9.8}Si_{38.2}O_{96}$	$Cs_{9.8}Al_{9.8}Si_{38.2}O_{96}\cdot 11CO_2$
Temperature/K	298	298	298	298
Space group	$I\bar{4}3m$	$I\bar{4}3m$	$I\bar{4}3m$	$Im\bar{3}m$
X-ray source	Beamline I11	Beamline I11	Cu	Cu
Diffractometer	Synchrotron	Synchrotron	PANalytical	PANalytical
Wavelength(s) (Å)	0.827159(2)	0.827159(2)	1.54056 1.54430	1.54056 1.54430
a/ Å	14.4139(6)	14.6513(6)	14.6287(6)	14.9960(1)
Volume/Å^3	2994.62(1)	3145.04(1)	3130.5(1)	3372(3)
R_p	0.0790	0.0807	0.0345	0.0236
R_{wp}	0.1067	0.1045	0.0454	0.0277
χ^2	2.533	5.453	2.223	1.814

	K-Rho	**K-Rho (0.5 bar CO_2)**	**K-Rho (1 bar CO_2)**	**K-Rho (heated after CO_2 adsorption)**
Unit cell	$K_{9.8}Al_{9.8}Si_{38.2}O_{96}$	$K_{9.8}Al_{9.8}Si_{38.2}O_{96}\cdot xCO_2$	$K_{9.8}Al_{9.8}Si_{38.2}O_{96}\cdot 11CO_2$	$K_{9.8}Al_{9.8}Si_{38.2}O_{96}$
Temperature/K	298	298	298	298
Space group	$I\bar{4}3m$	$I\bar{4}3m$	$I\bar{4}3m$	$I\bar{4}3m$
X-ray source	Beamline I11	Beamline I11	Beamline I11	Cu
Diffractometer	Synchrotron	Synchrotron	Synchrotron	PANalytical
Wavelengths (Å)	0.826956(2)	0.826956(2)	0.826956(2)	1.54056 1.54430
a/ Å	14.5959(3)	(I) 14.6612(7) (II) 14.7435(8)	14.7631(3)	14.6078(7)
Volume/Å^3	3109.54(5)	(I) 3151.41(1) (II) 3204.77(5)	3217.63(5)	3117.1(1)
R_p	0.0158	0.0211	0.0267	0.0639
R_{wp}	0.0233	0.0280	0.0187	0.0333
χ^2	5.002	17.190	18.170	4.147

	K-chabazite	**K-chabazite (1 bar CO_2)**
Unit cell	$K_9Al_9Si_{27}O_{72}$	$K_9Al_9Si_{27}O_{72}\cdot 9CO_2$
Temperature/K	298	298
Space group	$R\bar{3}m$	$R\bar{3}m$
X-ray source	Cu	Cu
Diffractometer	STOE	PANalytical
Wavelength(s) (Å)	1.54056	1.54056 1.54430
a/ Å	13.7242(7)	13.982(9)
c/ Å	14.630(4)	14.735(2)
Volume/Å^3	2386.5(8)	2495(8)
R_p	0.0888	0.0469
R_{wp}	0.1130	0.0624
χ^2	2.120	4.102

S6. Fractional atomic coordinates, occupancies and isotropic displacement parameters (in Å^2) and the Rietveld plots of Na-Rho, dehydrated and with adsorbed CO_2

Table S6

Na-Rho	x	y	z	Occup.	Multipl.	Uiso
Si1	0.2740(2)	0.1224(2)	0.4255(2)	0.8	48	0.0200(8)
Al1	0.2740(2)	0.1224(2)	0.4255(2)	0.2	48	0.0200(8)
O1	0.0386(3)	0.2106(3)	0.3866(4)	1	48	0.0200(8)
O2	0.2190(4)	0.2190(4)	0.4037(6)	1	24	0.0200(8)
O3	0.1159(4)	0.1159(4)	0.6296(4)	1	24	0.0200(8)
Na (S8R)	0.3850(1)	0	0	0.506(9)	12	0.0200(8)
Na (S6R)	0.3132(7)	0.3132(7)	0.3132(7)	0.433(2)	8	0.0200(8)

Na-Rho (1 bar)	x	y	z	Occup.	Mult.	Uiso
Si1	0.2676(2)	0.1174(2)	0.4181(2)	0.8	48	0.0115(6)
Al1	0.2676(2)	0.1174(2)	0.4181(2)	0.2	48	0.0115(6)
O1	0.0303(3)	0.2108(3)	0.3769(4)	1	48	0.0115(6)
O2	0.2101(4)	0.2101(4)	0.3928(7)	1	24	0.0115(6)
O3	0.1342(4)	0.1342(4)	0.6202(4)	1	24	0.0115(6)
Na (S6R)	0.3990(7)	0.3990(7)	0.3990(7)	0.490(1)	8	0.0286(3)
Na (S8R)	0.0183(1)	0.0183(1)	0.4426(1)	0.25	24	0.0286(3)
O(CO2)1a	0.3922(1)	0	0	0.5	12	0.068(7)
O(CO2)1b	0.2301(1)	0	0	0.5	12	0.068(7)
C(CO2)1	0.3106(1)	0	0	0.5	12	0.068(7)
O(CO2)2a	0.1337(1)	0.1337(2)	0.0505(1)	0.24983	24	0.068(7)
O(CO2)2b	0.1958(1)	0.1274(3)	0.1958(1)	0.24983	24	0.068(7)
C(CO2)2	0.1352(1)	0.1350(1)	0.1350(1)	0.74939	8	0.068(7)

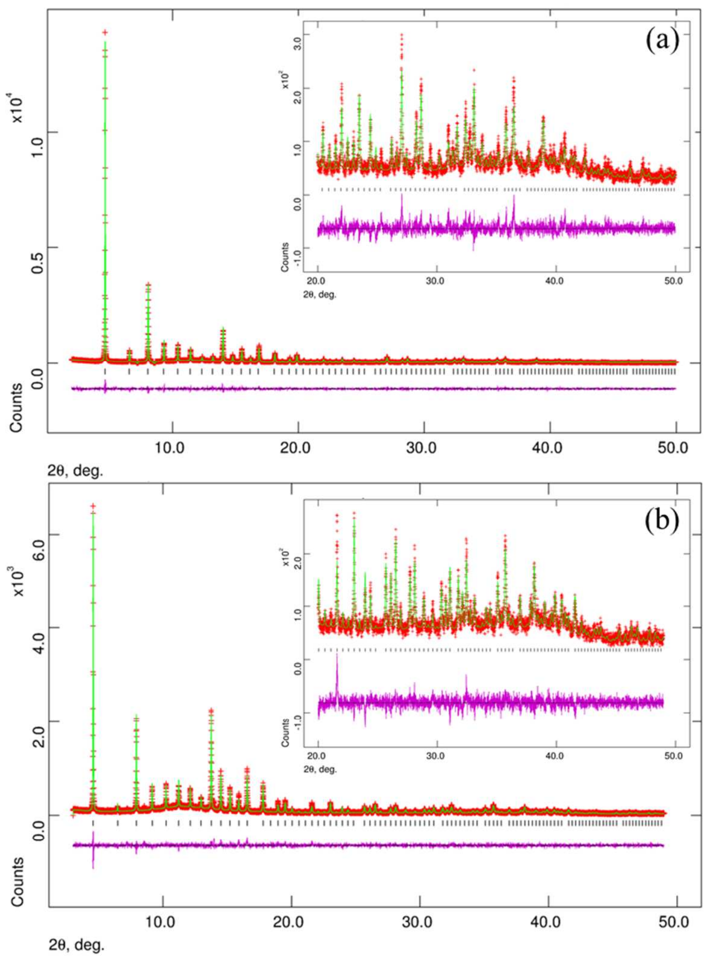

Figure S6.1 Final observed, calculated and difference Rietveld plots for the synchrotron powder data refinement (λ = 0.827159(2) Å) of (a) dehydrated Na-Rho and (b) Na-Rho in equilibrium with 1 bar of CO_2.

S7. Fractional atomic coordinates, occupancies and isotropic displacement parameters (in Å^2) of Cs-Rho dehydrated and with adsorbed CO_2

Table S7

Cs-Rho	**x**	**y**	**z**	**Occup.**	**Mult.**	**Uiso**
Si1	0.2696(3)	0.1205(2)	0.4198(2)	0.8	48	0.0110(2)
Al1	0.2696(3)	0.1205(2)	0.4198(2)	0.2	48	0.0110(2)
O1	0.0292(2)	0.2176(3)	0.3829(5)	1.0	48	0.0089(3)
O2	0.2092(4)	0.2092(4)	0.3946(6)	1.0	24	0.0089(3)
O3	0.1359(4)	0.1359(4)	0.6322(3)	1.0	24	0.0089(3)
Cs (D8R)	0.0	0.0	0.5	1.0	6	0.0416(1)
Cs (S6R)	0.1759(2)	0.1759(2)	0.1759(2)	0.440(3)	8	0.0416(1)

Cs-Rho (4 bar)	**x**	**y**	**z**	**Occup.**	**Mult.**	**Uiso**
Si1	0.25	0.1008(3)	0.3992(3)	0.8	48	0.0372(2)
Al1	0.25	0.1008(3)	0.3992(3)	0.2	48	0.0372(2)
O1	0.0	0.2191(5)	0.3828(5)	1.0	48	0.0372(2)
O2	0.1693(5)	0.1693(5)	0.3767(6)	1.0	48	0.0372(2)
Cs (S6R)	0.3536(4)	0.3536(4)	0.3536(4)	0.233(3)	16	0.0468(2)
Cs (S8R)	0.5	0.1486(4)	0.5	0.5	12	0.0468(2)
O(CO2)1a	0.4131(2)	0.0	0.0	0.5	12	0.0468(2)
O(CO2)1b	0.2537(2)	0.0	0.0	0.5	12	0.0468(2)
C(CO2)1	0.3334(2)	0.0	0.0	0.5	12	0.0468(2)
O(CO2)2a	0.4150(3)	0.510(4)	0.4150(3)	0.10	48	0.0468(2)
O(CO2)2b	0.3673(3)	0.654(4)	0.456(9)	0.05	96	0.0468(2)
C(CO2)2	0.3956(3)	0.583(4)	0.417(4)	0.10	48	0.0468(2)

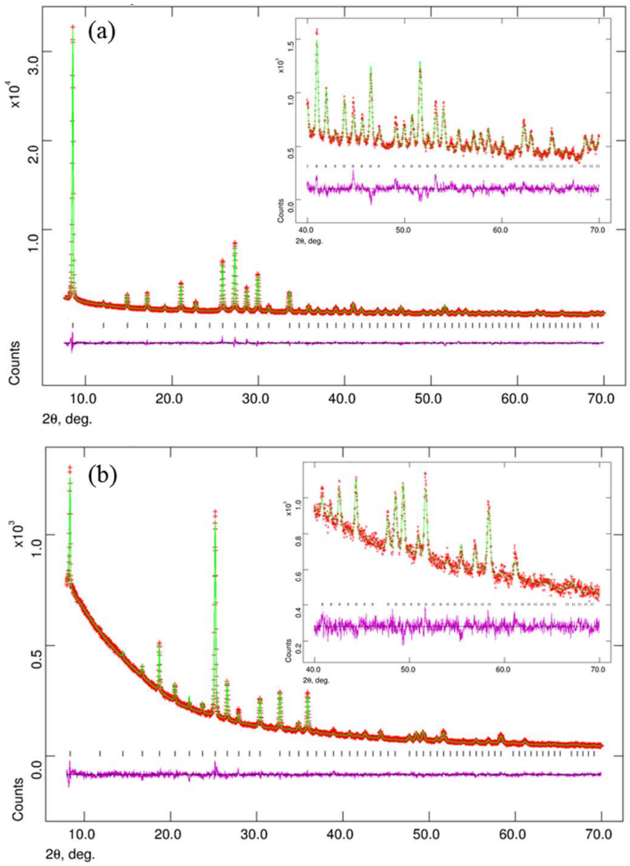

Figure 7.1 Final observed, calculated and difference Rietveld plots for the laboratory powder X-ray diffraction data refinement (λ_1 = 1.54056 Å, λ_2 =1.54430 Å) of (a) dehydrated Cs-Rho and (b) Cs-Rho in equilibrium with 4 bar of CO_2.

S8. In situ laboratory PXRD of K-Rho with adsorbed CO_2

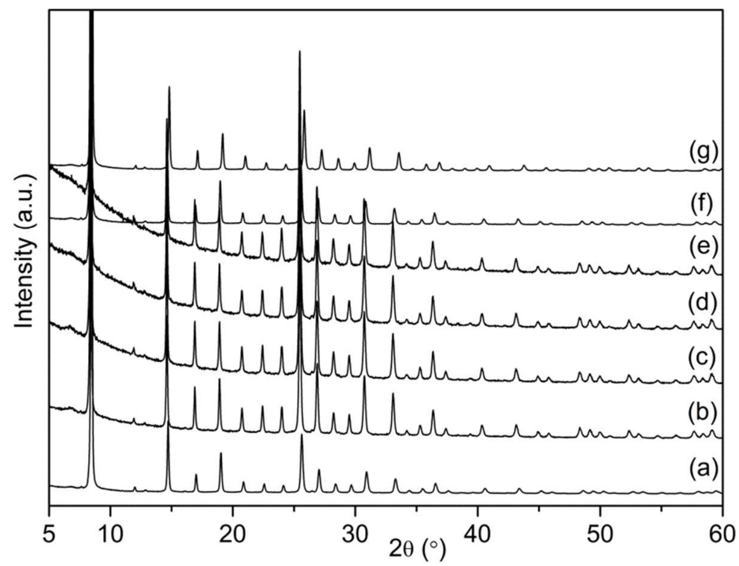

Figure S8.1 *In situ* laboratory PXRD (Cu $K_{\alpha1,\alpha2}$) of K-Rho during CO_2 adsorption up to 5 bar. (a) and (g) samples dehydrated at 573 K under He flux for 2 hours and cooled down to RT and samples in equilibrium with (b) 1 bar, (c) 2 bar, (d) 3 bar, (e) 4 bar, and (f) sample dehydrated at 298 K under He flux for 2 hours. The (offset) patterns have been collected at 298 K using the same operating conditions.

S9. Fractional atomic coordinates, occupancies and isotropic displacement parameters (in $Å^2$) of K-Rho dehydrated and with adsorbed CO_2: Rietveld plots of K-Rho dehydrated, with adsorbed CO_2 (0.5 bar, 1 bar) and with CO_2 removed.

Table S9

K-Rho	x	y	z	Occup.	Mult.	Uiso
Si1	0.2682(5)	0.1193(5)	0.4183(5)	0.8	48	0.0121(7)
Al1	0.2682(5)	0.1193(5)	0.4183(5)	0.2	48	0.0121(7)
O1	0.2094(1)	0.2094(1)	0.3971(2)	1.0	48	0.0121(7)
O2	0.1300(1)	0.1300(1)	0.6239(1)	1.0	24	0.0121(7)
O3	0.0278(1)	0.2088(8)	0.3863(1)	1.0	24	0.0121(7)
K (D8R)	0.5	0.0	0.0	0.2907(2)	6	0.0248(4)
K (S8R)	0.3610(2)	0.0	0.0	0.5976(2)	12	0.0547(2)
K (S6R)	0.3295(4)	0.3295(4)	0.3295(4)	0.1193(2)	8	0.0090(8)

K-Rho (0.5 bar, I)	x	y	z	Occup.	Mult.	Uiso
Si1	0.26837(2)	0.11941(2)	0.41735(2)	0.8	48	0.01295(3)
Al1	0.26837(2)	0.11941(2)	0.41735(2)	0.2	48	0.01295(3)
O1	0.20768(3)	0.20768(3)	0.4016(5)	1.0	48	0.01295(3)
O2	0.12436(3)	0.12436(3)	0.6274(4)	1.0	24	0.01295(3)
O3	0.02515(3)	0.21486(3)	0.38511(3)	1.0	24	0.01295(3)
K (S6R)	0.31686(4)	0.31686(4)	0.31686(4)	0.4328	8	0.01295(3)
K (S8R)	0.3644(5)	0.0	0.0	0.5	12	0.01295(3)
OC1	0.4294(9)	0.0	0.0	0.465(4)	12	0.06133
OC2	0.2402(9)	0.0	0.0	0.465(4)	12	0.06133
CO1	0.3369(1)	0.0	0.0	0.465(4)	12	0.06133
OC3	0.3347(8)	0.4615(1)	0.3347(8)	0.0411(2)	24	0.06133
OC4	0.3728(2)	0.6275(2)	0.3728(2)	0.123(6)	8	0.06133
CO2	0.3687(3)	0.5380(2)	0.3687(3)	0.0411(2)	24	0.06133

K-Rho (0.5 bar, II)	x	y	z	Occup.	Mult.	Uiso
Si1	0.26619(2)	0.11666(2)	0.41408(2)	0.8	48	0.01295(3)
Al1	0.26619(2)	0.11666(2)	0.41408(2)	0.2	48	0.01295(3)
O1	0.1991(4)	0.1991(4)	0.3977(6)	1.0	48	0.01295(3)
O2	0.1332(4)	0.1332(4)	0.6290(5)	1.0	24	0.01295(3)
O3	0.0238(4)	0.21063(3)	0.3761(4)	1.0	24	0.01295(3)
K (S6R)	0.3458(5)	0.3458(5)	0.3458(5)	0.4328	8	0.01295(3)
K (S8R)	0.3784(6)	0.0	0.0	0.5	12	0.01295(3)
OC1	0.4413(9)	0.0	0.0	0.5	12	0.06133
OC2	0.2609(9)	0.0	0.0	0.5	12	0.06133
CO1	0.3502(1)	0.0	0.0	0.5	12	0.06133
OC3	0.3631(1)	0.4926(1)	0.3631(1)	0.2	24	0.06133
OC4	0.3440(1)	0.6560(1)	0.3440(1)	0.6	8	0.06133
CO2	0.3641(1)	0.5802(2)	0.3641(1)	0.2	24	0.06133

K-Rho (1 bar)	x	y	z	Occup.	Mult.	Uiso
Si1	0.26624(7)	0.11655(8)	0.41504(8)	0.8	48	0.01142(2)
Al1	0.26624(7)	0.11655(8)	0.41504(8)	0.2	48	0.01142(2)
O1	0.20030(1)	0.20030(1)	0.39406(3)	1.0	48	0.01142(2)
O2	0.13504(2)	0.13504(2)	0.63192(2)	1.0	24	0.01142(2)
O3	0.02295(2)	0.21134(1)	0.37890(2)	1.0	24	0.01142(2)
K (S6R)	0.34714(2)	0.34714(2)	0.34714(2)	0.4328(3)	8	0.0312
K (S8R)	0.37326(3)	0.0	0.0	0.5	12	0.0312
OC1	0.4372(4)	0.0	0.0	0.5	12	0.0232(2)
OC2	0.3097(5)	0.0	0.0	0.5	12	0.0232(2)
CO1	0.1740(9)	0.0	0.0	0.5	12	0.0232(2)
OC3	0.3631(6)	0.5028(7)	0.3631(6)	0.2167	24	0.0232(2)
OC4	0.3401(4)	0.6599(4)	0.3401(4)	0.65	8	0.0232(2)
CO2	0.3529(8)	0.5903(1)	0.3529(8)	0.2167	24	0.0232(2)

K-Rho (heated to remove CO_2)	x	y	z	Occupancy	Mult.	Uiso
Si1	0.2688(1)	0.1192(2)	0.4185(2)	0.8	48	0.0189(7)
Al1	0.2688(1)	0.1192(2)	0.4185(2)	0.2	48	0.0189(7)
O1	0.2096(3)	0.2096(3)	0.4006(5)	1.0	48	0.0180(1)
O2	0.1305 (3)	0.1305(3)	0.6223(4)	1.0	24	0.0180(1)
O3	0.0307(3)	0.2102(2)	0.3854(3)	1.0	24	0.0180(1)
K (D8R)	0.5	0.0	0.0	0.310(5)	6	0.04083
K (S8R)	0.3659(5)	0.0	0.0	0.574(5)	12	0.06832
K (S6R)	0.3220(2)	0.3220(2)	0.3220(2)	0.093(8)	8	0.03901

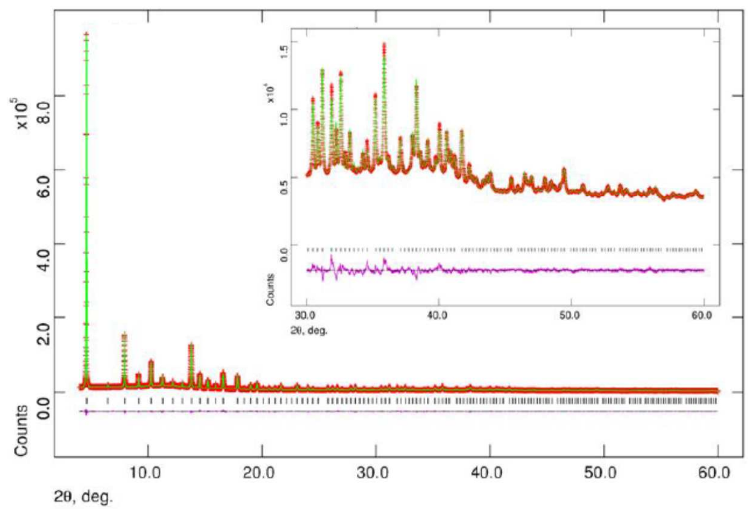

Figure S9.1 Final observed, calculated and difference Rietveld plots for the synchrotron powder X-ray diffraction data refinement (λ = 0.826956 Å) of dehydrated K-Rho.

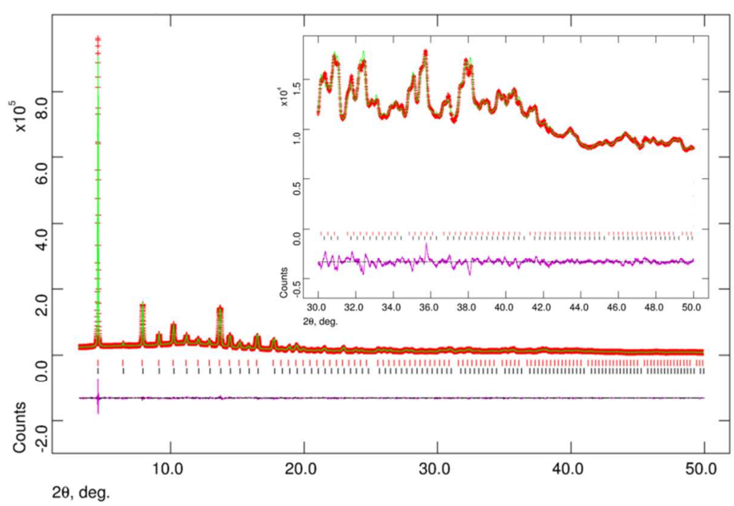

Figure S9.2 Final observed, calculated and difference Rietveld plots for the synchrotron powder X-ray data refinement (λ = 0.826956 Å) of K-Rho in equilibrium with 0.5 bar of CO_2. The profile was fitted using two phases of K-Rho, both I-43m symmetry, with different *a* parameters.

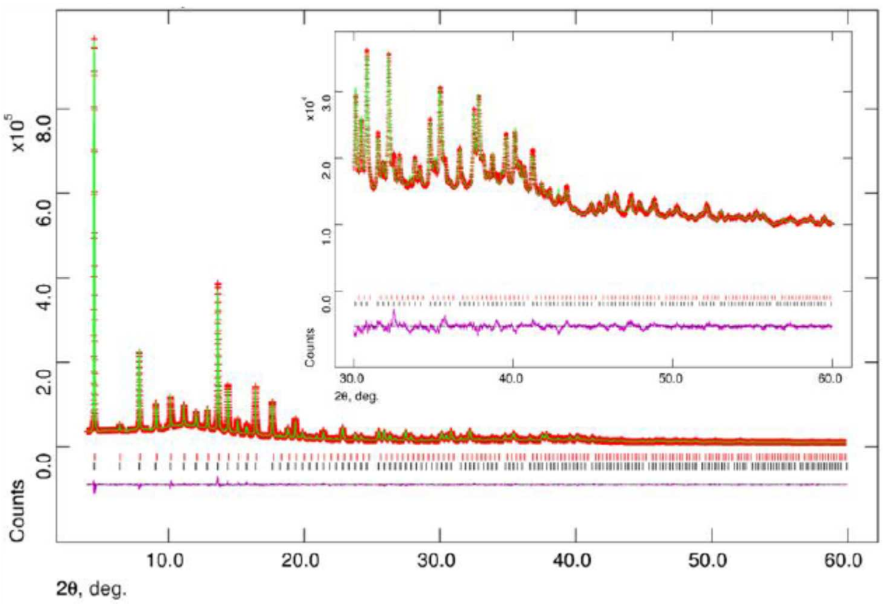

Figure S9.3 Final observed, calculated and difference Rietveld plots for the synchrotron PXRD data refinement (λ = 0.826956 Å) of K-Rho in equilibrium with 1 bar CO_2.

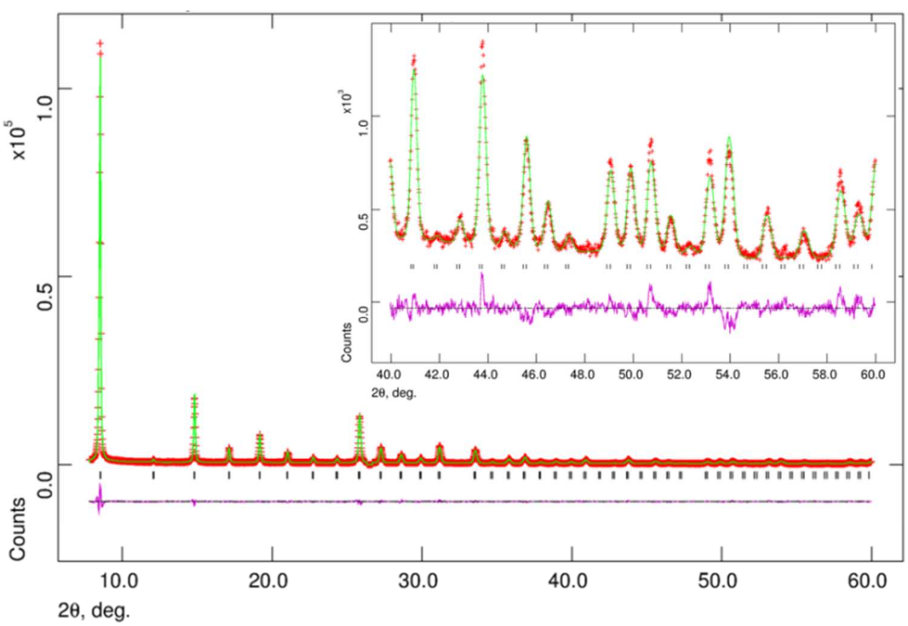

Figure S9.4 Final observed, calculated and difference Rietveld plots for the laboratory powder X-ray data refinement ($K\alpha_1$ = 1.54056 Å, $K\alpha_2$ =1.54430 Å) of K-Rho after adsorption of CO_2 and heating at 573 K in helium to remove all adsorbed CO_2.

S10. Cation positions in Na-, K- and Cs-Rho dehydrated and when in contact with CO_2

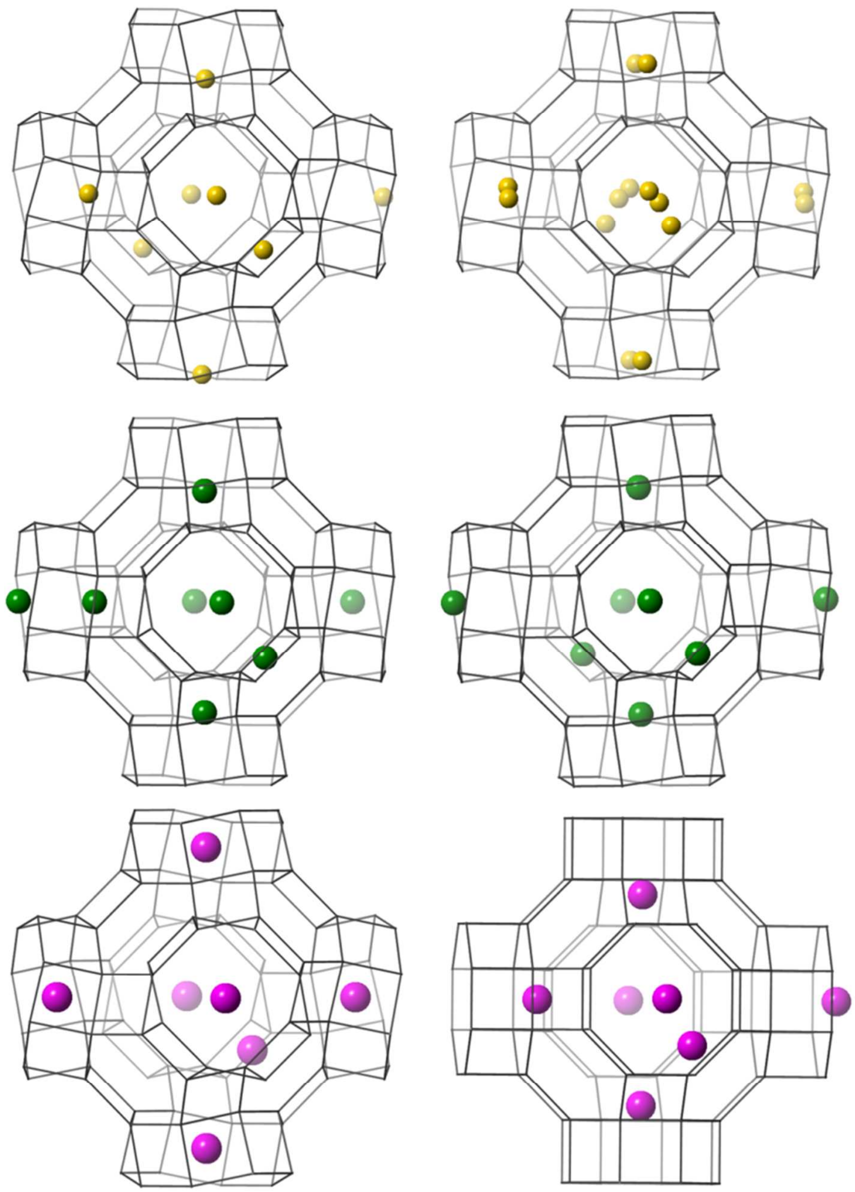

Figure S10.1 Plots showing (top) Na, (middle) K and Cs cation positions in cages of Rho (T-T linkages only shown) in (left) dehydrated structures and (right) when in contact with 1, 1 and 4 bar CO_2, respectively.

S11. Fractional atomic coordinates, occupancies and isotropic displacement parameters (in Å^2) of K-chabazite dehydrated and with adsorbed CO_2

Table S11

K-chabazite	**x**	**y**	**z**	**Occup.**	**Multipl.**	**Uiso**
Si1	0.9999(1)	0.2239(2)	0.1064(1)	0.75	36	0.0516(2)
Al1	0.9999(1)	0.2239(2)	0.1064(1)	0.25	36	0.0516(2)
O1	0.9058(3)	0.0942(3)	0.1247(4)	1.0	18	0.0417(3)
O2	0.9726(5)	0.3060(5)	0.1667(0)	1.0	18	0.0417(3)
O3	0.1225(2)	0.2448(4)	0.1354(3)	1.0	18	0.0417(3)
O4	0.0	0.2540(4)	0.0	1.0	18	0.0417(3)
K (S8R)	0.5	0.5	0.0	0.996(9)	9	0.1149(8)

K-chabazite (1bar)	**x**	**y**	**z**	**Occup.**	**Multipl.**	**Uiso**
Si1	1.0024(4)	0.2286(4)	0.1072(3)	0.75	36	0.023(4)
Al1	1.0024(4)	0.2286(4)	0.1072(3)	0.25	36	0.023(4)
O1	0.8990(5)	0.1010(5)	0.1275(9)	1.0	18	0.023(4)
O2	0.9793(8)	0.3127(8)	0.1667	1.0	18	0.023(4)
O3	0.1137(3)	0.2272(6)	0.1329(7)	1.0	18	0.023(4)
O4	0.0	0.2506(1)	0.0	1.0	18	0.023(4)
K (S8R)	0.5	0.5	0.0	0.5	9	0.002(7)
K (S6R)	0.0	0.0	0.2295(1)	0.662(1)	6	0.002(7)
C100	0.6879	0.1990	0.7556	0.288(5)	36	0.100(3)
O100	0.2046	0.5884	0.2185	0.288(5)	36	0.100(3)
O200	0.5818	0.4836	-0.0589	0.288(5)	36	0.100(3)

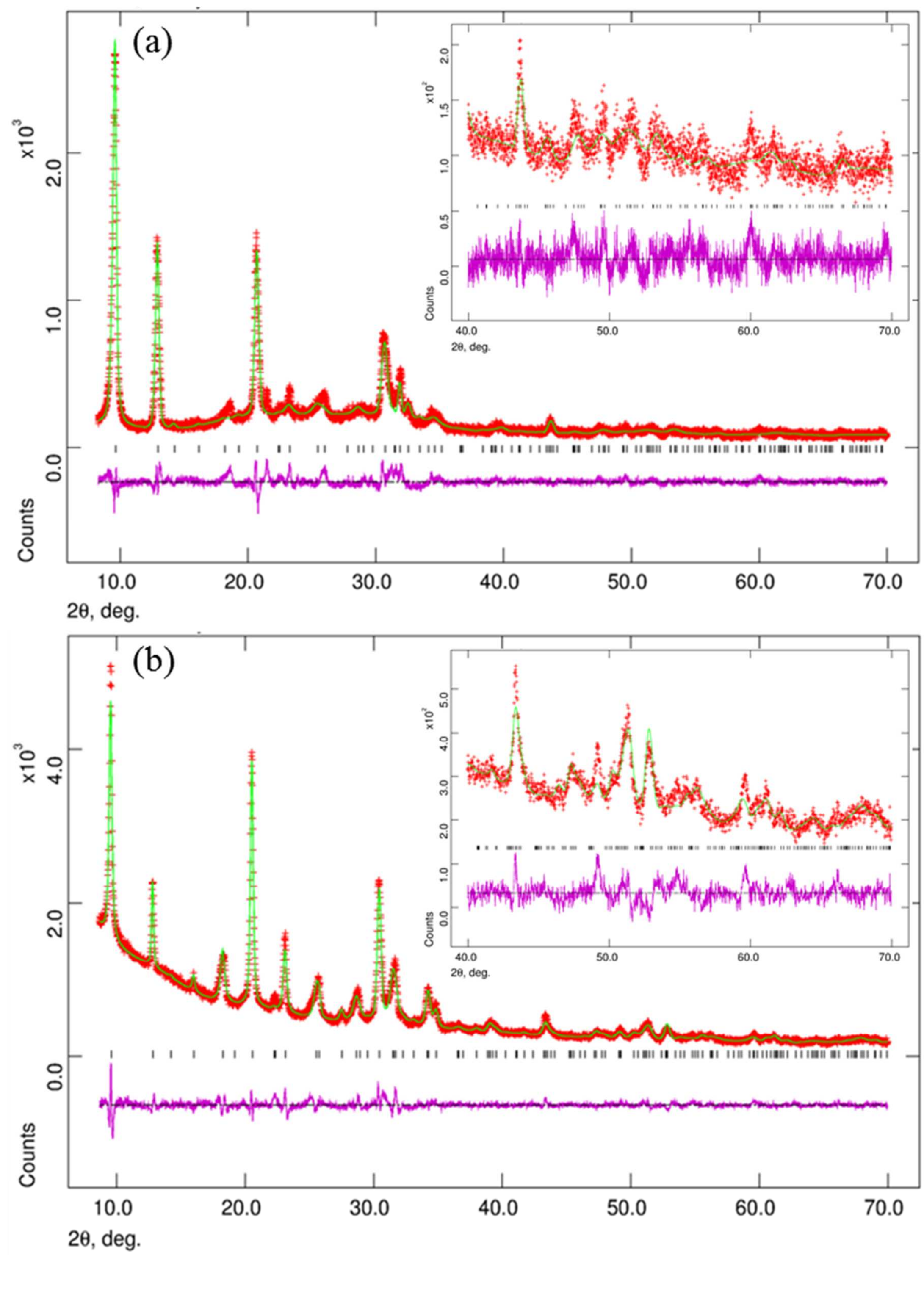

Figure S11.1 Final observed, calculated and difference Rietveld plots for the laboratory powder data refinement (λ_1 = 1.54056 Å, λ_2 =1.54430 Å) of (a) dehydrated K-chabazite and (b) K-chabazite in equilibrium with 1 bar of CO_2.

References

1. Chatelain T., Patarin J., Fousson E., Soulard M., Guth J. L. and Schulz P., *Microporous Mater.*, **1995**, *4*, 231-238
2. Lozinska M. M., Mangano E., Mowat J. P. S., Shepherd A. M., Howe R. F., Thompson S. P., Parker J. E., Brandani S. and Wright P. A., *J. Am. Chem. Soc.*, **2012**, *134*, 17628-17642
3. Zhang J., Singh R. and Webley P. A., *Micropor. Mesopor. Mat.*, **2008**, *111*, 478-487
4. Dyer A. and Enamy H., *Zeolites*, **1981**, *1*, 66-68
5. Lee Y., Reisner B. A., Hanson J. C., Jones G. A., Parise J. B., Corbin D. R., Toby B. H., Freitag A. and Larese J. Z., *J. Phys. Chem. B*, **2001**, *105*, 7188-7199
6. Langmi H. W., Book D., Walton A., Johnson S. R., Al-Mamouri M. M., Speight J. D., Edwards P. P., Harris I. R. and Anderson P. A., *J. Alloys Compd.*, **2005**, *404–406*, 637-642
7. Ridha F. N., Yang Y. and Webley P. A., *Micropor. Mesopor. Mat.*, **2009**, *117*, 497-507